Fatigue analysis of a post-buckled composite single-stringer specimen taking into account the local stress ratio

Raimondo, A.; Bisagni, C.

DOI
10.1016/j.compositesb.2020.108000

Publication date
2020

Document Version
Final published version

Published in
Composites Part B: Engineering

Composites Part B 193 (2020) 108000

Contents lists available at ScienceDirect

Composites Part B

journal homepage: www.elsevier.com/locate/compositesb

Fatigue analysis of a post-buckled composite single-stringer specimen taking into account the local stress ratio

A. Raimondo, C. Bisagni *

Faculty of Aerospace Engineering, Delft University of Technology, Delft, the Netherlands

ARTICLE INFO

Keywords:
Composite structures
Delamination
Skin-stringer separation
Fatigue
Post-buckling
Local stress ratio

ABSTRACT

The fatigue life prediction of post-buckled composite structures represents still an unresolved issue due to the complexity of the phenomenon and the high costs of experimental testing. In this paper, a novel numerical approach, called "Min-Max Load Approach", is used to analyze the behavior of a composite single-stringer specimen with an initial skin-stringer delamination subjected to post-buckling fatigue compressive load. The proposed approach, based on cohesive zone model technique, is able to evaluate the local stress ratio during the delamination growth, performing, in a single Finite Element analysis, the simulation of the structure at the maximum and minimum load of the fatigue cycle. The knowledge of the actual value of the local stress ratio is crucial to correctly calculate the crack growth rate. At first, the specimen is analyzed under quasi-static loading conditions, then the fatigue simulation is performed. The results of the numerical analysis are compared with the data of an experimental campaign previously conducted, showing the capabilities of the proposed approach.

1. Introduction

The potential of composite structures in the aerospace industry have not yet been fully exploited, especially in the post-buckling regime, due to the difficulties in controlling and predicting their complex failure mechanisms. Indeed, typical aeronautical composite stiffened panels can work in the post-buckling regime, but the prediction of their collapse mode becomes quite complex, as it is due to the interaction of the post-buckling deformation with different failure modes, such as intralaminar damage, delamination, skin-stringer separation [1,2]. The phenomenon is even more complex for fatigue loading conditions, due to the interaction between the geometric nonlinearities of the response, the different possible damage modes, and the accumulation of cyclic damage.

Delamination, and in particular in the form of skin-stringer separation, is among the most critical types of damage in stiffened panels, as it can be difficult to predict and can rapidly grow under the appropriate conditions.

Despite the large number of studies, the simulation of interlaminar damage in composite structures subjected to fatigue load is still an open question. Delamination growth is usually treated as a crack propagation problem, and most of the existing numerical approaches make use of methodologies originated for metallic materials, such as the Paris law [3], which is widely used to characterize experimental data in terms of crack growth rate versus the variation of the energy release rate or the stress intensity factor during the load cycle [4]. In the last decades, a variety of numerical techniques have been developed with the aim to integrate the Paris law in the framework of a Finite Element (FE) analysis. The Virtual Crack Closure Technique (VCCT) has been employed by several authors [5–8] to evaluate the energy release rate and therefore the crack growth rate using the Paris law. The methodology has been recently introduced in the FE code ABAQUS [9] and has proven to provide good results in analyzing fatigue-driven delamination at the coupon level [10,11]. On the other hand, Cohesive Zone Model (CZM) approaches use interface elements positioned along the surface in which the crack is expected to growth. Approaches based on CZM have been widely used to simulate delamination in composite laminates subjected to static or impact loads [12–15], and recently have been extended by some authors to take into account degradation due to cyclic load by incorporating the Paris law within the cohesive constitutive model [16–21].

In the simulation of crack propagation for constant amplitude fatigue loading conditions, both VCCT and CZM approaches are usually implemented with the so called "envelope load method" [22]. This technique allows to avoid the simulation of the load oscillation during each fatigue cycle by modelling only the maximum load and keeping it

* Corresponding author.
E-mail address: c.bisagni@tudelft.nl (C. Bisagni).

https://doi.org/10.1016/j.compositesb.2020.108000
Received 30 January 2020; Received in revised form 20 March 2020; Accepted 21 March 2020
Available online 31 March 2020

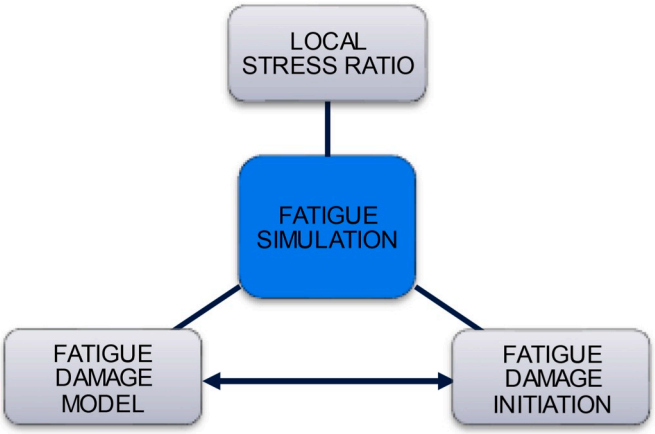

Fig. 1. Main aspects of the ongoing research work on fatigue simulation.

constant. The load variation is taken into account within the damage model using a scalar parameter, the applied load ratio, which is defined as the ratio between the minimum and maximum applied load during the fatigue cycle ($R_{Applied} = P_{min}/P_{max}$).

This represents a strong limitation of the numerical models based on the load envelope approach since the crack growth rate evaluated with the Paris law only depends on the local stress ratio, that is the ratio between the minimum and maximum value of the stress at the crack tip or, alternatively, the square root of the ratio between the minimum and the maximum value of the energy release rate ($R_{Local} = \sigma_{min}/\sigma_{max} = [G_{min}/G_{max}]^{0.5}$), and therefore it is essential to know its value to correctly simulate fatigue crack propagation [23]. To overcome this limitation, a numerical approach, called "Min-Max Load Approach", has been developed to evaluate the local stress ratio during a fatigue analysis [24,25]. The methodology has been validated using experimental results of Double Cantilever Beam (DCB) and Mixed-Mode Bending (MMB) specimens and then applied to a specimen equal to the MMB but with different loading conditions able to create a variable local stress ratio.

In this work, the "Min-Max Load Approach" is applied to a single-stringer specimen with an initial skin-stringer separation, subjected to fatigue compressive loads [26]. The Single-Stringer Compression (SSC) specimen was designed to capture the behavior of large multi-stringer panels, typical of fuselage structures [27–29]. This specimen is relatively small, computationally tractable yet detailed numerical models can be constructed to account for all damage modes associated with multi-stringer panels. Despite its small size, the specimen displays a relative high level of complexity, allowing the study of failure behavior in the post-buckling regime and providing data to verify quasi-static and fatigue numerical models thanks to its limited dimensions which make it computationally feasible.

In section 2, the research context of this work is introduced, while in section 3 the "Min-Max Load Approach" is described and the adopted cohesive fatigue damage formulation is briefly summarized. In section 4, the numerical results of quasi-static and fatigue analysis performed on the SSC specimen are presented and compared to experimental data.

2. Fatigue life of post-buckled composite structures

The work presented in this paper is part of a research effort with the objective of developing a numerical methodology for the prediction of fatigue-life of aeronautical composite structures in the post-buckling regime. In particular, the main interest is the initiation and propagation of delamination and skin-stringer separation in composite stiffened panels under cyclic loads. Although several approaches existent in literature are able to simulate fatigue damage propagation at the coupon level, in most cases they are not yet suitable for application to component or full-scale structure. The ongoing research work is focusing on

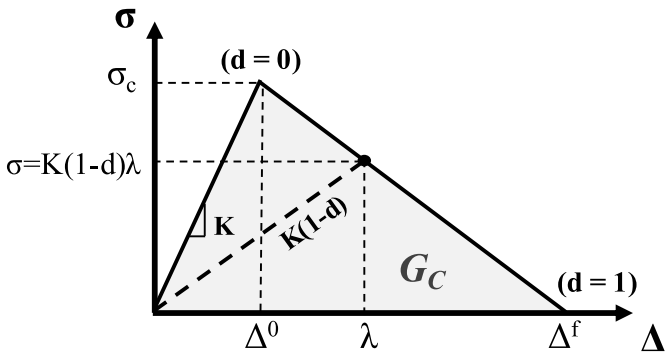

Fig. 2. Bilinear traction-separation law.

three different but connected aspects needed for a correct simulation of the fatigue behavior of post-buckled composite structures: the evaluation of the local stress ratio, the definition and implementation of a new damage constitutive model and the development of a fatigue damage initiation criterion (Fig. 1).

As stated in the introduction, most of the available numerical models are based on the envelope load method, where the local stress ratio is assumed to be equal to the applied load ratio along the crack front during the propagation of the damage. However, especially for the analysis of structures in the post-buckling regime, this hypothesis is proven not to be applicable and numerical approaches able to take this phenomenon into account are needed. To address this issue, a methodology, called "Min-Max Load Approach" is developed to calculate the local stress ratio during a fatigue analysis and is described in this paper.

Regarding the fatigue damage model, most of the formulations based on cohesive elements depend on parameters that have to be determined by calibration and comparison with experimental results and are only valid for specific load ratio and mode-mixity. A novel fatigue constitutive model able to overcome these issues is currently under development and will be later combined with the "Min-Max Load Approach". Since the proposed methodology for the evaluation of the local stress ratio can be used together with any fatigue damage model, an existing model taken from literature is employed in this paper, introducing some modifications required to implement the numerical approach.

Finally, although cohesive elements are in principle capable of modelling fatigue damage initiation, there is no established methodology or criterion in literature able to predict the occurrence of fatigue damage in a pristine structure. Different approaches are currently under consideration to identify the location of fatigue damage initiation where cohesive elements have to be placed and to estimate the number of cycles needed for the damage to propagate.

The integration of these three different approaches in a single numerical methodology will allow to take a significant step towards the developing of cohesive model based numerical tools. These tools will help in reducing the number of tests required for the design and certification of structures in composite materials able to work safely in the post-buckling regime.

3. Theoretical background

In this section, at first, the theoretical background of the cohesive constitutive model for quasi-static and fatigue crack propagation analysis adopted in the proposed numerical methodology is summarized together with the modifications needed to calculate the crack growth rate in presence of variable local stress ratio. Then, the idea and the actual implementation of the "Min-Max Load Approach" for the evaluation of the local stress ratio are described in detail.

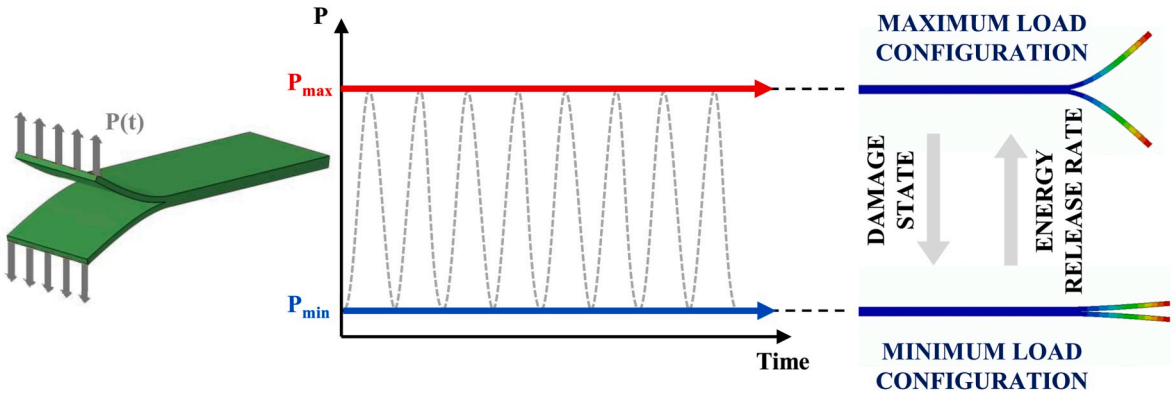

Fig. 3. "Min-Max Load Approach" applied to a Double Cantilever Beam.

3.1. Fatigue cohesive model

Cohesive elements have been widely used to model delamination propagation under quasi-static or impact loading conditions. A bilinear traction-separation law is assumed, where the stress at the interface follows a linear increase up to the interface strength of the material, σ_c, and then starts to decrease up to the complete failure of the element. The area under the traction-separation law represents the critical energy release rate of the material, G_c. The constitutive response is graphically illustrated in Fig. 2.

The interface degradation is driven by a damage parameter which depends on the opening displacements of the cohesive element, as shown in equation (1):

$$d = \frac{\Delta^f(\lambda - \Delta^0)}{\lambda(\Delta^f - \Delta^0)} \tag{1}$$

where λ is the cohesive equivalent displacement, Δ^0 is the damage onset displacement and Δ^f is the cohesive displacement at failure. The scalar damage parameter, d, represents the overall damage in the material and is related to the ratio between the dissipated energy due to the damage and the fracture toughness of the material.

In presence of fatigue loading conditions, the constitutive model can be extended taking into account the variation of the damage parameter with the number of cycles which can be expressed as a sum of a quasi-static damage rate ($\partial d_s/\partial N$) and a fatigue damage rate ($\partial d_f/\partial N$) as illustrated in equation (2):

$$\frac{\partial d}{\partial N} = \frac{\partial d_s}{\partial N} + \frac{\partial d_f}{\partial N} \tag{2}$$

The term related to the damage created by static overloads ($\partial d_s/\partial N$) develops according to equation (1), while several formulations can be found in literature for the calculation of the fatigue damage rate ($\partial d_f/\partial N$). As stated in the previous section, for the purpose of this work the choice of the constitutive model is not relevant since the proposed methodology can be integrated with any cohesive fatigue formulation. In this work, the following equation is adopted [17]:

$$\frac{\partial d_f}{\partial N} = \frac{1}{l_{CZ}} \frac{[\Delta^f(1-d) + d\Delta^0]^2}{\Delta^f \Delta^0} \frac{da}{dN} \tag{3}$$

where l_{CZ} is the length of the cohesive zone and da/dN is the crack growth rate.

The crack growth rate is evaluated using a semi-empirical fatigue delamination growth law which allows, with a single formula and three independent material parameters, to calculate the crack growth rate taking into account changes in the mode-mixity and in the local stress ratio [30]. The main assumption is that the local stress ratio and the mode-mixity only affect the slope of the crack growth rate curve (da/dN) as a function of the normalized energy release rate (G_{max}/G_c), as shown in equation (4):

$$\frac{da}{dN} = C\left[\frac{G_{\max}}{G_C(\varphi)}\right]^{\frac{b_{0I}}{(1-R_{Local})^{1+\alpha(\varphi)}} e^{-h\varphi}} \tag{4}$$

where C, b_{0I} and h are material dependent parameters, φ is the mode-mixity ($\varphi = G_{IImax}/G_{max}$) and G_{max} is the peak value of the energy release rate, defined as the sum of the maximum value of energy release rate mode I (G_{Imax}) and mode II (G_{IImax}):

$$G_{\max} = G_{I\max} + G_{II\max} \tag{5}$$

The parameter $\alpha(\varphi)$ is function of the mode-mixity and of the fracture toughness $G_C(\varphi)$:

$$\alpha(\varphi) = \frac{G_C(\varphi) - G_{IC}}{G_{IIC} - G_{IC}} \tag{6}$$

The mixed-mode fracture toughness is evaluated using the formula proposed by Benzeggangh and Kenane [31]:

$$G_C(\varphi) = G_{IC} + (G_{IIC} - G_{IC})\varphi^{\eta} \tag{7}$$

where η is an experimentally determined coefficient.

A cycle-jump strategy is employed in the fatigue model to save computational resources, meaning that not all the cycles of the loading history are simulated. The increment in the damage parameter after a cycle-jump can be calculated as reported in equation (8):

$$d^J_{i+\Delta N_i} = d^J_i + \frac{\partial d^J_i}{\partial N}\Delta N_i \quad with \quad \Delta N_i = \frac{\Delta d_{\max}}{\max_J\left\{\frac{\partial d^J_i}{\partial N}\right\}} \tag{8}$$

where $d^J_{i+\Delta Ni}$ is the damage variable at integration point J at cycle $N_{i+\Delta Ni}$, d^J_i is the damage variable at integration point J at cycle N_i, $\partial d^J_i/\partial N$ is the damage rate at integration point J at cycle N_i evaluated using equation (3), and ΔN_i is the number of cycles that can be jumped. The value of ΔN_i is calculated to ensure that the maximum increment in the damage variable among all the integration points after each cycle jump is below Δd_{max}, a parameter defined by the user, representing the sensitivity of the analysis.

3.2. Min-Max Load Approach

The analysis of fatigue crack propagation under constant amplitude loads is usually performed using the envelope load method which consists in simulating a constant load equal to the maximum load during the fatigue cycle and taking into account the load variation within the damage model using the applied load ratio. The main assumption in using this approach is that the stress state at the crack tip changes,

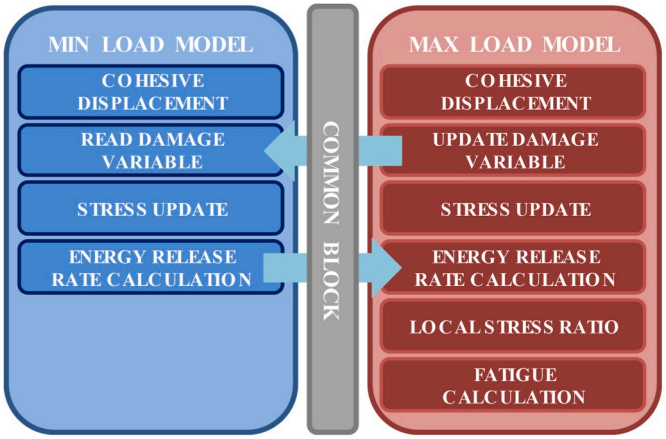

Fig. 4. Flowchart of the operations within the UMAT subroutine.

during each load cycle, in exactly the same way as the applied load. This implies that the local stress ratio is equal to the applied load ratio. While this assumption could be realistic for fatigue crack propagation in some cases, there are several situations where the applied load ratio differs from the local stress ratio, which can also change during the crack propagation and along the delamination front [23]. As an example, when a stiffened panel oscillates between pre- and post-buckling conditions during the fatigue cycle, due to the large variation of the panel deformed shape between the minimum and maximum load, the value of the local stress ratio is not equal to the applied load ratio and cannot be predicted in advance.

The proposed numerical methodology called "Min-Max Load Approach" allows to evaluate the local stress ratio during a fatigue crack propagation analysis. To calculate the local stress ratio it is necessary to know the stress state of the structure when it is subjected to the maximum and to the minimum load of the fatigue cycle. In this methodology, a single FE analysis with two identical models representing the same structure but with different constant applied loads is performed. One model analyzes the structure with the applied load equal to the minimum value of the fatigue cycle, while the other one the structure at the maximum load. The two FE models are discretized so that each element belonging to one configuration, the maximum or the minimum load, has the same element number of the corresponding element on the other configuration, with a constant offset. This technique allows to identify during the analysis to which model the element belongs. The main idea of the approach, applied to a DCB specimen, is schematically illustrated in Fig. 3.

The two models exchange information between each other to evaluate the local stress ratio and to perform the fatigue calculation. In particular, the minimum value of the energy release rate at the crack tip due to external loading is extracted from the model subjected to the minimum load during the fatigue cycle and is transferred to the model representing the structure at the maximum load. The knowledge of the minimum and maximum value of the energy release rate allows to calculate the local stress ratio for each element on the delamination front and to evaluate the crack growth rate using equation (4). The crack growth rate is then related to the increment in the damage variable of the cohesive elements using a fatigue cohesive model. Indeed, one of the advantages of the proposed approach is that it can be used in conjunction with any constitutive model. Once the fatigue calculations are performed, the increment in the damage state of the cohesive elements is

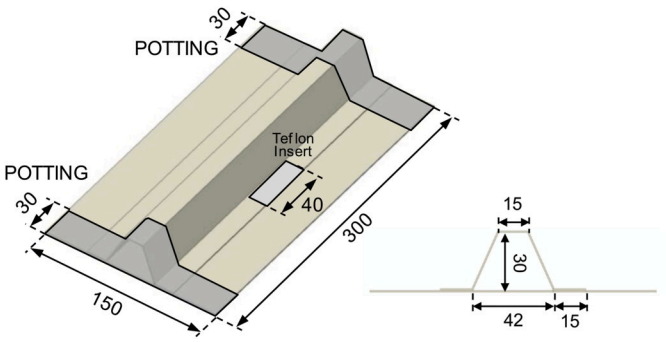

Fig. 5. Single-stringer compression specimen: geometry (dimensions in mm).

sent to the elements of the minimum load configuration to ensure that both models have the same representation of the crack.

The "Min-Max Load Approach" is implemented inside the FE code ABAQUS using a User Material Subroutine (UMAT) [9], written in Fortran language, which allows to define a completely user-defined material behavior and to share the information between the two models. The flowchart of the operations performed within the UMAT is shown in Fig. 4.

During the analysis for each load increment, at first, the element number of the integration point under consideration is used to identify to which model the element belongs. If the element is part of the minimum load configuration, after the cohesive displacements are updated, the value of the damage parameter is acquired from the corresponding element in the other configuration, the stresses are updated and the calculation of the energy release rate is performed. If, on the contrary, the element is part of the maximum load configuration, the damage variable and the stresses are updated, then the energy release rate is calculated and, using the minimum value of the energy release rate taken from the corresponding element of the other configuration, the local stress ratio is evaluated and used to perform the calculation of the crack growth rate using equation (4). The exchange of variables between the two models is carried out using a COMMON BLOCK, a Fortran-specific tool which allows to transfer information between subroutines.

The methodology has been preliminarily validated in Refs. [24,25] for fatigue crack propagation under pure mode I and mixed-mode conditions performing numerical simulations on 2D plane strain models of DCB and MMB specimens. It has then been adopted to analyze a specimen similar to the MMB but with modified loading conditions such as to produce a variable local stress ratio different from the applied load ratio. Comparisons with an analytical model based on the corrected beam theory have demonstrated the ability of the approach to predict the local stress ratio and the fatigue damage propagation without providing any information on the applied load ratio in the constitutive model. The developed "Min-Max Load Approach" is extended here to 3D cohesive elements to enable the simulation of fatigue crack propagation in a larger specimen with a higher degree of complexity subjected to cyclic compressive loads between pre- and post-buckling conditions, the SSC specimen. This is the type of application in which the knowledge of the local stress ratio is crucial for the evaluation of the crack growth rate.

4. Single-stringer compression specimen

The numerical approach described in the previous section is applied here to analyze a SSC specimen with an initial skin-stringer delamination. At first, the geometrical and FE models are introduced, and the results of a quasi-static analysis are presented. Then, the "Min-Max Load

Table 1
Material properties of IM7/8552.

Property	Unit	Value
E_1	[MPa]	150,000
E_2	[MPa]	9080
G_{12}	[MPa]	5290
N_{12}		0.32
G_{1C}	[kJ/m^2]	0.277
G_{2C}	[kJ/m^2]	0.788
η		1.63

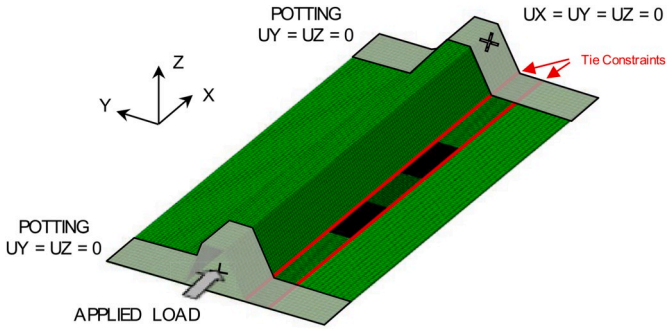

Fig. 6. Single-stringer compression specimen: finite element model and boundary conditions.

Approach" is adopted to simulate the evolution of the skin-stringer separation when the specimen is subjected to a cyclic load between pre- and post-buckling condition. For both quasi-static and fatigue analyses, the numerical results are compared with data of an experimental campaign previously conducted.

4.1. SSC specimen description and FE model

The SSC specimen consists of a skin co-cured with an omega-shaped stringer. An initial delamination is induced in the center of the specimen using a Teflon film placed between the skin and a stringer flange during manufacturing. The geometrical characteristics of the specimen are displayed in Fig. 5.

The skin is made of 8 plies of carbon-epoxy IM7/8552 with the stacking sequence $[45/90/-45/0]_s$, while the stringer has 7 plies with the layup [-45/0/45/0/45/0/-45]. The ply thickness is 0.125 mm. The material properties taken from Ref. [29] and adopted in the numerical analyses are shown in Table 1.

The SSC specimen is discretized in the FE code ABAQUS [9] using continuum shell elements (SC8R) with a size of approximately 2 mm. A layer of zero-thickness cohesive elements (COH3D8) is placed in the areas potentially involved in the delamination growth between the skin and the stringer flange where the Teflon film is located. In the initially delaminated region where the Teflon film is located, no cohesive element is positioned while a contact condition is enforced between the skin and the stringer flange to avoid elements compenetration. A finer discretization is adopted in a 40 mm region on the upper and lower side of the skin-stringer separation with an element length of 0.05 mm in the propagation direction. To reduce the total number of elements and decrease the computational times, the stringer flange and the portion of the skin below the stringer flange where the Teflon film is located are connected to the surrounding part of the structure using tie constraints.

Two references points, one at each end of the specimen, are defined and rigidly connected to the nodes located on the edges to uniformly apply the load. All the degrees of freedom are blocked for the reference points on the encased end of the specimen, while on the opposite end the specimen is allowed to move only along the longitudinal axis. The potting is numerically simulated constraining the lateral and out-of-plane displacements of the nodes and allowing them to move along the axial direction. The details of the FE model and the boundary conditions are illustrated in Fig. 6.

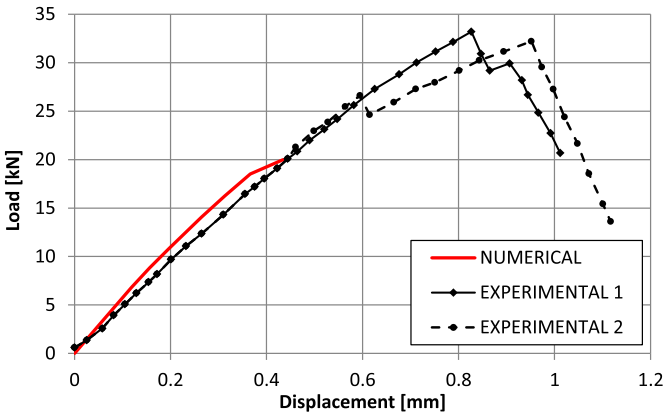

Fig. 7. Comparison between numerical and experimental quasi-static load-displacement curves.

The nodal coordinates of the model are perturbed using the displacements obtained from an eigenvalue buckling analysis. The displacements are scaled to a maximum value of 0.01 mm and added to the nodal coordinates to promote a smooth transition through the buckling bifurcation point and to avoid convergence issues.

4.2. Quasi-static analysis

At first, a quasi-static analysis is performed applying a compressive load to the reference point. The force versus displacement curve is presented in Fig. 7 and compared with the experimental data [29].

The trend of the numerical results in Fig. 7 is similar to the experimental data, although the predicted stiffness is slightly higher and the maximum load is lower. These differences may be due to a combination of multiple factors, such as the geometrical imperfections of the test specimens, the alignment of the loaded surfaces or the boundary conditions assumed for the potting. Furthermore, the interface properties adopted in the numerical analysis are experimentally evaluated according to the ASTM standard using DCB or MMB specimens with delamination positioned between 0° plies, while, in the tested specimens, the skin-stringer separation is located between −45° and 45° plies, resulting in much higher values of the fracture toughness.

In the numerical analysis, the skin-stringer delamination starts to propagate around an applied load of 18.5 kN. After this point the propagation rapidly becomes unstable and the analysis terminates at 20 kN when the delamination reaches the boundary of the finer cohesive elements area. In Fig. 8, the out-of-plane displacements at different applied loads are presented together with the damage state of the cohesive elements at the end of the quasi-static analysis.

Comparing Fig. 8a and b, it can be observed how, due to the propagation of the skin-stringer delamination, the skin is forced to buckle in a single half-wave mode, while in the opposite side the skin buckles in a three half-waves mode. The growth of the delamination is not symmetrical but rather tends to grow more on the upper side, as it can be noted in Fig. 8c where the cohesive elements completely damaged are reported in red.

4.3. Fatigue analysis

The experimental fatigue tests performed on the SSC specimen in

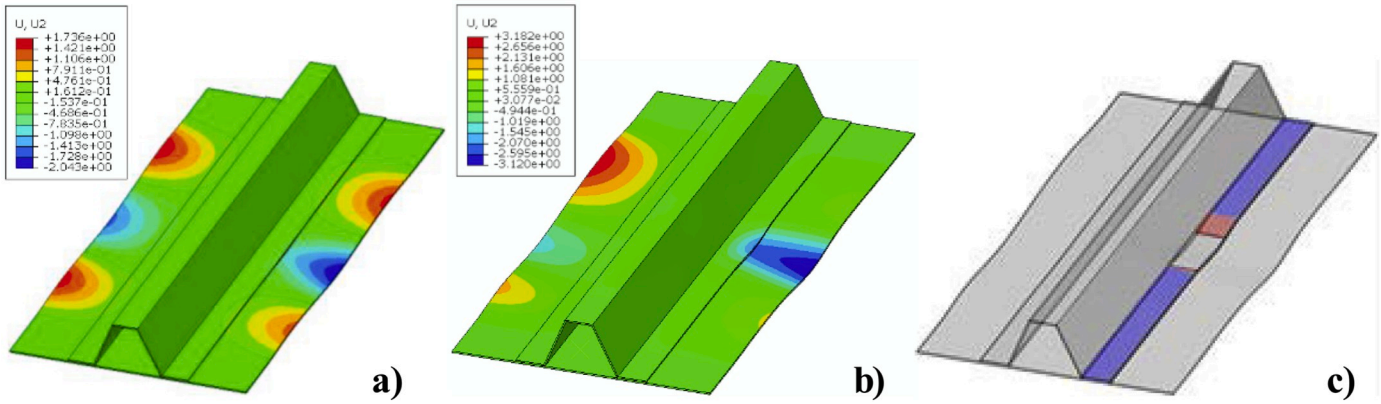

Fig. 8. Out-of-plane displacements of SSC specimen at: a) 16.5 kN; b) 20 kN. c) Cohesive damage state at 20 kN.

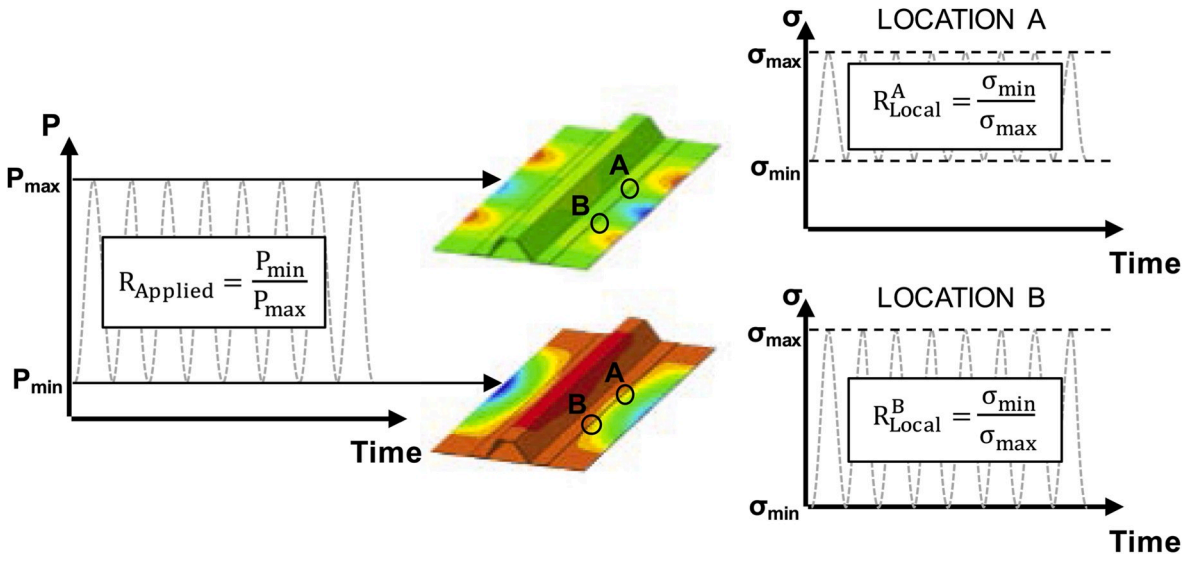

Fig. 9. Applied load ratio and local stress ratio in two locations along the delamination front.

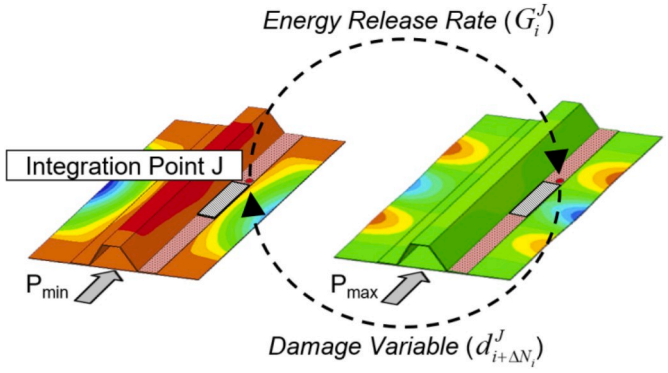

Fig. 10. "Min-Max Load Approach" applied to the SSC specimen.

Ref. [29] were conducted cycling the specimen between pre- and post-buckling conditions. The reason why the "Min-Max Load Approach" is essential for the analysis of this problem is graphically illustrated in Fig. 9.

Two points A and B located on the delamination front of the skin-stringer separation, due to the changing in deformed shape in the post-buckling regime, locally experience two different load oscillations. This results in two different local stress ratio both different from the applied load ratio. It is evident that using the applied load ratio to calculate the crack growth rate would results in an incorrect prediction of the damage propagation. Indeed, the local stress ratio is not only different for each point along the crack front, but it changes during the analysis due to the propagation of the delamination which modifies the post-buckling shape of the specimen. On the other hand, the applied load ratio is constant and its value is not equal to the local stress ratio in any point.

Table 2
Fatigue parameters for IM7/8552.

Parameter	Unit	Value
C	[mm]	3.51E-2
b_{OI}		14.05
h		1.47

The experimental fatigue tests were conducted cycling the specimen between 2.3 kN and 23 kN. The same load cycle cannot be adopted in the numerical analysis otherwise the maximum load would exceed the numerical quasi-static ultimate load, resulting in a complete separation of the skin from the stringer in the first load cycle. For this reason, the numerical fatigue analysis is performed with a maximum load of 18 kN, right before the beginning of the unstable propagation in the quasi-static analysis, and an applied load ratio of 0.1.

The "Min-Max Load Approach" is implemented discretizing two

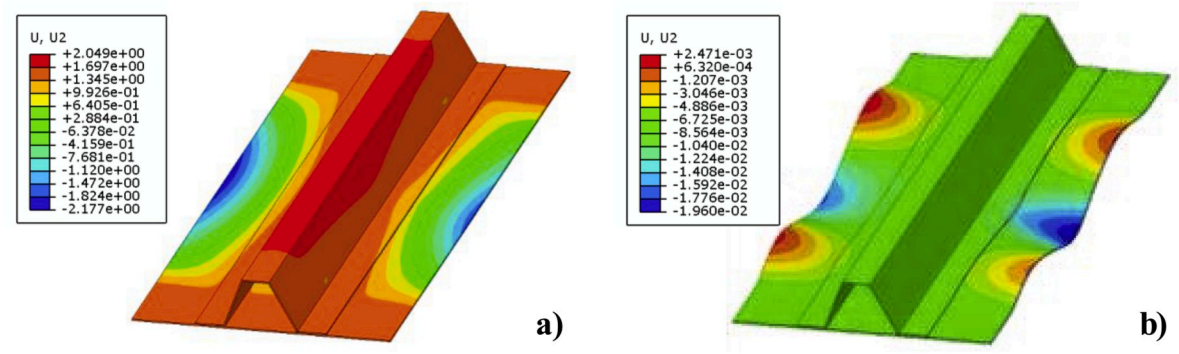

Fig. 11. Out-of-plane displacements: a) minimum load configuration (pre-buckling - 1.8 kN); b) maximum load configuration (post-buckling - 18 kN).

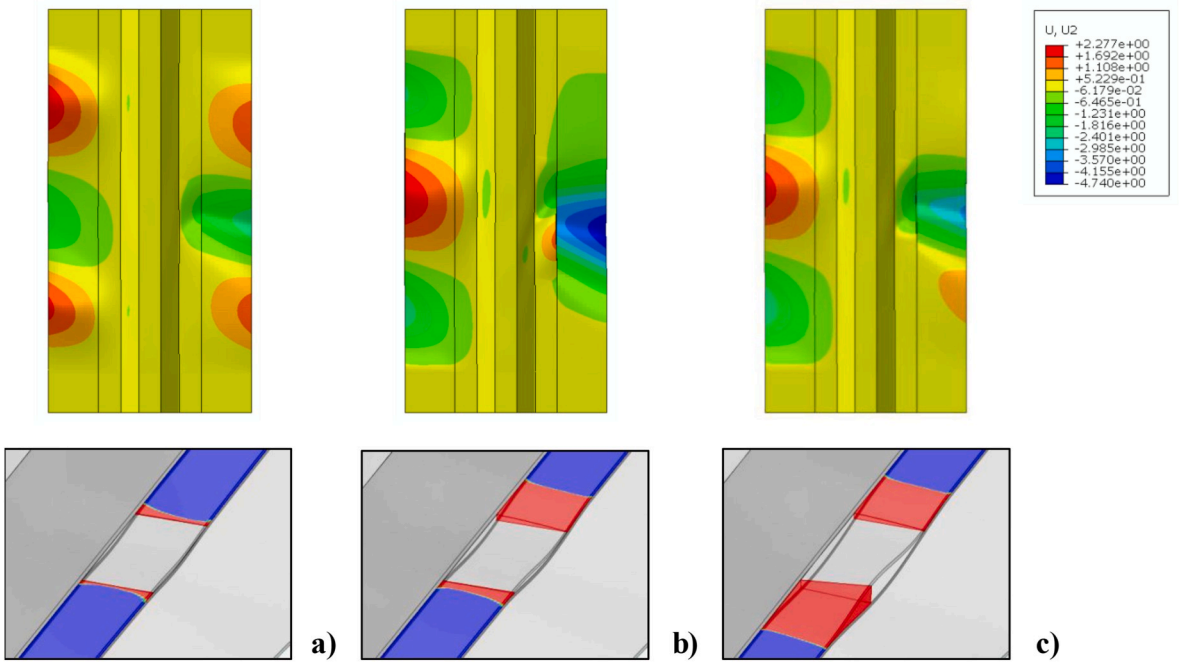

Fig. 12. Out-of-plane displacements at maximum load and delamination front after: a) 5000 cycles; b) 7800 cycles; c) 8100 cycles.

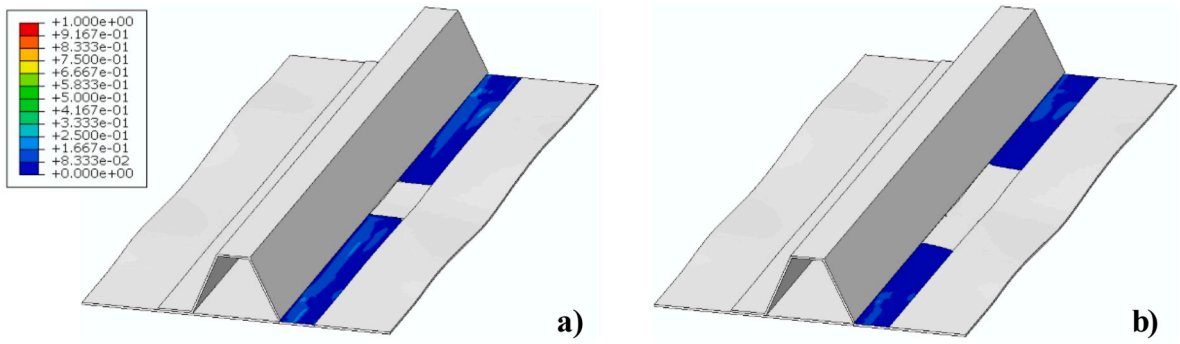

Fig. 13. Distribution of the state variable related to the local stress ratio at: a) first cycle; b) 10,000 cycles.

identical models of the SSC specimen, one subjected to the maximum and one to the minimum load of the fatigue cycle. The sequence of operations performed during the analysis, according to the procedure described in section 3.2, is graphically explained in Fig. 10.

The fatigue parameters adopted to calculate the crack growth rate according to equation (4) are taken from literature and reported in Table 2 [30].

In Fig. 11 the deformed shapes of the two configurations are shown at the beginning of the fatigue analysis.

The specimen oscillates between pre- and post-buckling conditions in each load cycle. During the simulation, as the skin-stringer separation advances, the out-of-plane displacements increase and the specimen jumps through different buckling modes. The deformed shapes of the maximum load configuration with the out-of-plane displacements

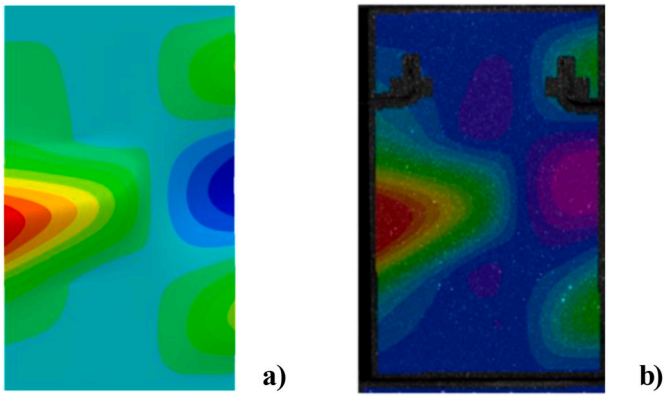

Fig. 14. Comparison between numerical and experimental out-of-plane displacements: a) Min-Max Load Approach at 10,000 cycles; b) digital image correlation at 11,850 cycles.

contour plot are shown with the corresponding evolution of the skin-stringer separation in Fig. 12 at different load cycles.

Initially (Fig. 12a), the skin buckles in three half-waves mode on both sides of the specimen. After about 7800 cycles (Fig. 12b) the portion of the skin on the opposite side of the delamination reverses its buckling direction, while under the delamination the skin starts to shift into a single half-wave mode. Then, at around 8100 cycles (Fig. 12c) the growth of the delamination between skin and stringer causes the stringer flange to snap from a single half-wave mode to a two half-waves buckling mode.

The propagation of the delamination is clearly affected by the sequence of buckling events which themselves are influenced by the growth of the delamination. The delamination grows slowly in the first 7000 cycles, then, the changes in the buckling mode shape leads to an increase in the crack growth rate. The analysis is terminated after 10,000 cycles because at that point one of the delamination fronts has reached the end of the refined cohesive zone.

During the fatigue analysis, within the UMAT, the value of the local stress ratio for each cohesive element is stored in a state variable. In Fig. 13, the distribution of the state variable corresponding to the local stress ratio is shown at the first cycle and at the end of the analysis, after 10,000 cycles.

Since the specimen oscillates between pre- and post-buckling conditions during the fatigue cycle, the cohesive stress is almost zero in the minimum load configuration and then the local stress ratio is close to zero. Without using the "Min-Max Load Approach" it would not have been possible to capture this behavior and a constant value of 0.1 equal to the applied load ratio would have been assumed for all the cohesive elements throughout all the analysis.

Comparisons in terms of deformed shape and delamination length with experimental digital image correlation data and ultrasonic scan taken from the skin side of the specimen are reported in Fig. 14 and Fig. 15, respectively.

In Fig. 14, the numerical out-of-plane displacement distribution at the end of the fatigue analysis can be qualitatively compared to the experimental observations. The side of the skin where the delamination is located buckles in a large single half-wave shape due to the propagation of the skin-stringer delamination, while on the opposite side the skin presents a three-half waves mode shape. The comparison with experimental data shows an excellent agreement in terms of post-buckling mode shape.

In Fig. 15, the final length of the skin-stringer delamination predicted by the numerical simulation, compared with the value measured experimentally, shows that the developed approach is able to capture the evolution of the damage propagation, although it should be taken into account that the numerical analysis is performed at a lower maximum load with respect to the experimental test. Clearly, for a real comparison it is necessary to improve the quasi-static model by experimentally characterizing the interface between the skin and the stringer.

5. Conclusions

In this paper, the behavior of a single-stringer composite specimen with an initial delamination subjected to post-buckling compressive fatigue load has been numerically investigated using an innovative approach, called "Min-Max Load Approach". The methodology, in a single finite element analysis, simulates the structure at the maximum and minimum load of the fatigue cycle, allowing to capture the actual value of the local stress ratio. The results of the numerical analysis have proven to be consistent with the data obtained from an experimental campaign previously performed, showing the potentialities of the proposed approach, although the numerical simulation has been conducted at a lower maximum load with respect to the experimental test. Further experimental data is required to correctly characterize the quasi-static and fatigue damage propagation of the considered interface.

Declaration of competing interest

The authors declare that they have no known competing financial interests or personal relationships that could have appeared to influence the work reported in this paper.

CRediT authorship contribution statement

A. Raimondo: Conceptualization, Methodology, Writing - review & editing. **C. Bisagni:** Conceptualization, Methodology, Writing - review & editing.

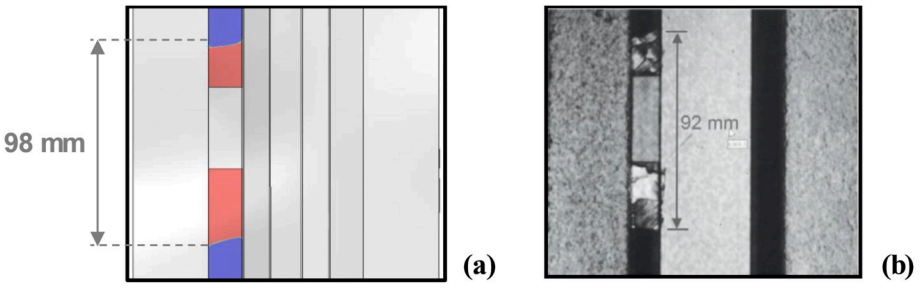

Fig. 15. Comparison between numerical and experimental damage propagation: a) Min-Max Load Approach at 10,000 cycles; b) ultrasonic scan at 11,850 cycles.

Acknowledgments

This work is sponsored by the Office of Naval Research (ONR), under grant award number N62909-17-1-2129. The views and conclusions contained herein are those of the authors only and should not be interpreted as representing those of ONR, the U.S. Navy or the U.S. Government.

The authors would like to thank Dr. Carlos Dávila from NASA Langley Research Center for his invaluable suggestions.

References

[1] Bisagni C, Vescovini R, Dávila CG. Development of a single-stringer compression specimen for the assessment of damage tolerance of postbuckled structures. J Aircraft 2011;48(2):495–502.
[2] Anyfantis KN, Tsouvalis NG. Post buckling progressive failure analysis of composite laminated stiffened panels. Appl Compos Mater 2012;19(3–4):219–36.
[3] Paris PC, Gomez MP, Anderson WE. A rational analytic theory of fatigue. Trend Eng 1961;13(9):9–14.
[4] Yao L, Sun Y, Guo L, Jia L, Zhao M. A validation of a modified Paris relation for fatigue delamination growth in unidirectional composite laminates. Compos B Eng 2018;132:97–106.
[5] Krueger R. Development of a benchmark example for delamination fatigue growth prediction. July 2010. Tech. Rep. NASA/CR-2010-216723. NASA.
[6] Riccio A, Ronza F, Sellitto A, Scaramuzzino F. Modeling delamination growth in composite panels subjected to fatigue load. Key Eng Mater 2015;627:21–4.
[7] De Carvalho NV, Mabson GE, Krueger R, Deobald LR. A new approach to model delamination growth in fatigue using the Virtual Crack Closure Technique without re-meshing. Eng Fract Mech 2019;222. https://doi.org/10.1016/j.engfracmech.2019.106614.
[8] Mabson GE, Deobald LR, Dopker B, Hoyt DM, Baylor JS, Graesser DL. Fracture interface elements for static and fatigue analysis. In: Proceedings of 16th international conference on composite materials (ICCM16), Kyoto; July 2007.
[9] Abaqus Analysis Guide. Dassault Systemes. 2019.
[10] Di Memmo I, Bisagni C. Fatigue simulation for damage propagation in composite structures. In: Proceedings of 32nd technical conference of the American society for composites, West Lafayette; October 2017. Paper number 135472.
[11] Raimondo A, Doesburg SA, Bisagni C. Numerical study of quasi-static and fatigue delamination growth in a post-buckled composite stiffened panel. Compos B Eng 2019. https://doi.org/10.1016/j.compositesb.2019.107589.
[12] Camanho PP, Dávila CG, de Moura M. Numerical simulation of mixed-mode progressive delamination in composite materials. J Compos Mater 2003;37:1415–38.
[13] Iarve EV, Gurvich MR, Mollenhauer DH, Rose CA, Dávila CG. Mesh-independent matrix cracking and delamination modeling in laminated composites. Int J Numer Methods Eng 2011;88:749–73.
[14] Riccio A, Raimondo A, Di Caprio F, Fusco M, Sanità P. Experimental and numerical investigation on the crashworthiness of a composite fuselage sub-floor support system. Compos B Eng 2018;150:93–103.
[15] Tuo H, Lu Z, Ma X, Zhang C, Chen S. An experimental and numerical investigation on low-velocity impact damage and compression-after-impact behavior of composite laminates. Compos B Eng 2019;167:329–41.
[16] Landry B, LaPlante G. Modeling delamination growth in composites under fatigue loadings of varying amplitudes. Compos B Eng 2012;43(2):533–41.
[17] Turon A, Costa J, Camanho PP, Dávila CG. Simulation of delamination in composites under high-cycle fatigue. Compos Appl Sci Manuf 2007;38(11):2270–82.
[18] Pirondi A, Giuliese G, Moroni F. Fatigue debonding three-dimensional simulation with cohesive zone. J Adhes 2016;92(7–9):553–71.
[19] Harper PW, Hallett SR. A fatigue degradation law for cohesive interface elements - development and application to composite materials. Int J Fatig 2010;32(11):1774–87.
[20] Robinson P, Galvanetto U, Tumino D, Bellucci G, Violeau D. Numerical simulation of fatigue-driven delamination using interface elements. Int J Numer Methods Eng 2005;63:1824–48.
[21] Moreira RDF, de Moura MFS, Silva FGA, Reis JP. High-cycle fatigue analysis of adhesively bonded composite scarf repairs. Compos B Eng 2020;190. https://doi.org/10.1016/j.compositesb.2020.107900.
[22] Bak BLV, Sarrado C, Turon A, Costa J. Delamination under fatigue loads in composite laminates: a review on the observed phenomenology and computational methods. Appl Mech Rev 2014;66(6):1–24.
[23] Krueger R, Deobald L, Mabson GE, Engelstad S, Rao MP, Gurvich M, Seneviratne W, Perera S, O'Brien TK, Murri G, Ratcliffe J, Dávila CG, De Carvalho N. Guidelines for VCCT-based interlaminar fatigue and progressive failure finite element analysis. 2017. NASA/TM–2017-219663.
[24] Raimondo A, Bisagni C. A numerical approach for the evaluation of the local stress ratio in fatigue-driven delamination analysis. In: Proceeding of AIAA Scitech 2019 Forum. San Diego; January 2019. Paper number 6.2019-1545.
[25] Raimondo A, Bisagni C. Analysis of local stress ratio for delamination in composites under fatigue loads. AIAA J 2019. https://doi.org/10.2514/1.J058465.
[26] Bisagni C. Fatigue life of post-buckled composite structures. In: Proceedings of 22nd International Conference on Composite Materials (ICCM22). Melbourne; August 2019.
[27] Bisagni C, Dávila CG. Experimental investigation of the postbuckling response and collapse of a single-stringer specimen. Compos Struct 2014;108:493–503.
[28] Davila CG, Bisagni C. Fatigue life and damage tolerance of postbuckled composite stiffened structures with indentation damage. J Compos Mater 2018;52(7):931–43.
[29] Dávila CG, Bisagni C. Fatigue life and damage tolerance of postbuckled composite stiffened structures with initial delamination. Compos Struct 2017;161:73–84.
[30] Allegri G, Wisnom MR, Hallett SR. A new semi-empirical law for variable stress-ratio and mixed-mode fatigue delamination growth. Compos Appl Sci Manuf 2013;48:192–200.
[31] Benzeggagh ML, Kenane M. Measurement of mixed-mode delamination fracture toughness of unidirectional glass/epoxy composites with mixed-mode bending apparatus. Compos Sci Technol 1996;56:439–49.